




RESEARCH ARTICLE

Seasonal ground ice impacts on spring ecohydrological conditions in a western boreal plains peatland

Brandon Van Huizen¹  | Richard M. Petrone¹  | Jonathan S. Price¹  |
William L. Quinton²  | John W. Pomeroy³ 

¹Department of Geography & Environmental Management, University of Waterloo, Waterloo, ON, Canada

²Cold Regions Research Centre, Wilfrid Laurier University, Waterloo, ON, Canada

³Centre for Hydrology, University of Saskatchewan, Saskatoon, SK, Canada

Correspondence

Brandon Van Huizen, Department of Geography & Environmental Management, University of Waterloo, 200 University Ave West, Waterloo, ON, Canada.
Email: bvanhuizen@uwaterloo.ca.

Funding information

Natural Sciences and Engineering Research Council of Canada; Suncor Energy Incorporated; Boreal Water Futures; Shell Canada Energy; Imperial Oil Resources Limited; Suncor Energy Inc.; National Science and Engineering Research Council (NSERC)

Abstract

Peatlands in the Western Boreal Plains act as important water sources in the landscape. Their persistence, despite potential evapotranspiration (PET) often exceeding annual precipitation, is attributed to various water storage mechanisms. One storage element that has been understudied is seasonal ground ice (SGI). This study characterized spring SGI conditions and explored its impacts on available energy, actual evapotranspiration, water table, and near surface soil moisture in a western boreal plains peatland. The majority of SGI melt took place over May 2017. Microtopography had limited impact on melt rates due to wet conditions. SGI melt released 139mm in ice water equivalent (IWE) within the top 30cm of the peat, and weak significant relationships with water table and surface moisture suggest that SGI could be important for maintaining vegetation transpiration during dry springs. Melting SGI decreased available energy causing small reductions in PET (<10mm over the melt period) and appeared to reduce actual evapotranspiration variability but not mean rates, likely due to slow melt rates. This suggests that melting SGI supplies water, allowing evapotranspiration to occur at near potential rates, but reduces the overall rate at which evapotranspiration could occur (PET). The role of SGI may help peatlands in headwater catchments act as a conveyor of water to downstream landscapes during the spring while acting as a supply of water for the peatland. Future work should investigate SGI influences on evapotranspiration under differing peatland types, wet and dry spring conditions, and if the spatial variability of SGI melt leads to spatial variability in evapotranspiration.

KEYWORDS

evapotranspiration, ground heat flux, microtopography, peatlands, seasonal ground ice, western boreal plain

Abbreviations: AET, Actual Evapotranspiration; AOSR, Alberta Oil Sands Region; EC, Eddy Covariance; IDW, Inverse Distance Weighting; IWE, Ice Water Equivalent; MF, Mid Fen; NTF, North Treed Fen; PET, Potential Evapotranspiration; PETQG₁₀, Calculated potential evapotranspiration assuming the ground heat flux is 10% of net radiation; PETQG_{Cal}, Calculated potential evapotranspiration using the calorimetric ground heat flux; PETQG_{none}, Calculated potential evapotranspiration ignoring ground heat flux; Q_G, Ground Heat Flux; Q_G_L, Latent Heat Flux component; Q_G_S, Sensible Heat Flux component; SGI, Seasonal Ground Ice; SWE, Snow Water Equivalent; VMC, Volumetric Moisture Content; WBP, Western Boreal Plain.

1 | INTRODUCTION

Peatlands are ubiquitous in the Western Boreal Plain (WBP) (Petrone, Silins, & Devito, 2007), persisting in the landscape despite the presence of a subhumid climate where annual potential evapotranspiration (PET) often exceeds annual precipitation (Devito, Creed, & Fraser, 2005; Marshall, Schut, & Ballard, 1999). Peatlands in the WBP serve as important carbon storage features (Gorham, 1991; Kleinen, Brovkin, & Schuldt, 2012) and water sources for ecosystems within this landscape (Thompson, Mendoza, Devito, & Petrone, 2015). Peatland persistence can be attributed to the dynamic nature of their physical properties (Waddington et al., 2015; Whittington & Price, 2006), which keep the peatland surface in close proximity to the water table maintaining the wet conditions required for peat accumulation. However, during the spring (e.g., March–June), water losses from peatlands can be enhanced by the presence of thick seasonal ground ice (SGI) due to a reduction in storage capacity, which increases surface run-off (Price & Fitzgibbon, 1987; Woo & Winter, 1993). SGI can also persist well into the growing season (Brown, Petrone, Mendoza, & Devito, 2010; Goodbrand, Westbrook, & van der Kamp, 2018; Petrone, Devito, & Silins, 2008; Thompson & Waddington, 2013), which extends its potential ecohydrological impacts.

SGI differs from permafrost because it melts within a year of its formation, generally occurring soon after ground surface temperatures are $\leq 0^{\circ}\text{C}$. The warmer peatland surface underlying cooler air creates a temperature gradient resulting in a transfer of energy from the ground via conduction (Hayashi, Goeller, Quinton, & Wright, 2007) and radiation (Hayashi, 2013; Oke, 1987), leading to the freezing of water within the peat pore spaces.

SGI represents a frozen soil state (van Everdingen, 1975) and exists in two forms: reticulate and concrete (Woo & Winter, 1993). Reticulate SGI forms in the unsaturated zone, from water present at the time of freezing or from moisture migration to the freezing front (Lunardini, 1981). Concrete SGI in peatlands forms at the interface of the unsaturated zone and the water table and freezes downwards into the saturated zone increasing the SGI thickness. The initial thickness of the ice is controlled both by the air temperature and the presence of a snowpack. As the snowpack develops, freezing slows down and stops (Moore, 1987) due to the insulative properties of the snowpack. SGI thickness can also increase from above during periodic melt events. When an overlying snowpack begins to melt, snowmelt reaches the base of the snowpack and can refreeze upon contact with the frozen ground surface (Granger, Gray, & Dyck, 1984; Nagare, Schincariol, Quinton, & Hayashi, 2012; Redding & Devito, 2011).

SGI reduces peatland infiltrability due to ice filled pore spaces. Reticulate ice in the unsaturated zone only has a minor impact during the spring due to the presence of air in larger pore spaces (Price, 1987; Smerdon & Mendoza, 2010). The greater impact on peatland infiltrability and storage capacity is the position of the concrete SGI relative to the peatland surface, which can vary with micro-topography. When concrete SGI forms close to the ground surface, it

reduces the spring snowmelt infiltration rate (Hayashi, 2013), creating a transient perched water table and surface ponding. The impervious nature of concrete SGI is due to the large storage capacity of peat in the near surface layers. Total porosity in the top 20 cm for peatlands in the WBP can range from 0.94 to 0.98 (Redding & Devito, 2005), which means the water content in the near surface peat can range from 94% to 98%. Thus, when concrete SGI forms in peatlands, it is predominantly ice, with little peat material, resulting in a soil layer that is effectively impervious to large amounts of infiltration.

By restricting the infiltration of snowmelt water, concrete SGI increases snowmelt run-off (Price, 1987; Price & FitzGibbon, 1987), an important recharge source in the WBP landscape (Smerdon, Mendoza, & Devito, 2008). Therefore, SGI can promote a peatlands ability to act as a source of water within the WBP landscape. The resulting increase in ponded water and surface saturation also allows for actual evapotranspiration (AET) near PET rates, even during the lower available energy conditions of the spring period (Brown et al., 2010; Petrone et al., 2008). However, snowmelt run-off and evaporated water reduce the amount of water entering peatland storage, increasing the reliance on precipitation and groundwater inputs for peatlands to maintain an adequate moisture supply during the snow free period. Melt water released from melting SGI is not an additional water input into the peatland, because it is a function of the antecedent moisture conditions prior to freezing. However, where this freezing occurs during winter may help keep water closer to the surface for the following spring. During the spring, *Sphagnum* mosses, the dominant peat forming vegetation (Hayward & Clymo, 1982) for bogs and poor fens, are typically close to their optimal moisture content (Moore et al., 2006). Consequently, the absence of SGI in the spring, when combined with a thin snowpack or minimal precipitation, may reduce the resiliency of surface vegetation to moisture stress.

Snowmelt run-off and AET water losses are in part due to the physical presence of SGI. However, the presence of melting SGI means more energy is driving phase change compared with temperature change. When including this phase change in the ground heat flux (Q_G) calculation, it increases Q_G , which can reduce available energy for evapotranspiration. The Q_G can be partitioned (Rouse, 1984) into a sensible (Q_{G_s}) and a latent (Q_{G_l}) heat flux. For SGI to melt, a substantial amount of energy is required to drive the phase change due to the high latent heat of fusion of ice (334 J/g; Farouki, 1981). This increases the Q_{G_l} component of Q_G , increasing the total Q_G (Runkle, Wille, Gazovic, Wilmking, & Kutzbach, 2014; Woo & Xia, 1996), which reduces available energy at the surface for evapotranspiration (Lafleur, McCaughey, Joiner, Bartlett, & Jelinski, 1997; Rouse, 2000). Despite high moisture conditions supplied by snow and SGI melt near the surface promoting conditions where AET is close to PET (Petrone, Devito, Silins, Mendoza, et al., 2008), SGI also has the potential to reduce peatland water losses during the spring. Whether SGI enhances or reduces water losses from the peatland surface is dependent on available moisture and energy during melt, which is controlled by the melt rate.

When SGI is at or close to the peatland surface, melt rates of SGI depend on the energy transfer across the peatland surface, which is

controlled by the peat thermal characteristics. A higher proportion of air relative to liquid water in the soil (e.g., hummocks) results in a lower thermal conductivity, and the SGI melt rates may be slower (Kingsbury & Moore, 1987). A higher proportion of liquid water relative to air (e.g., hollows) means melt rates can increase due to the higher thermal conductivity of water (McClymont, Hayashi, Bentley, & Christensen, 2013). Therefore, peatland microtopography may influence SGI melt rates and subsequently horizontal and vertical water losses. Yet the influence of microtopography on SGI melt and whether SGI melt significantly increases or decreases evapotranspiration has not been studied in depth. The role of SGI on hydrological processes in WBP peatlands, particularly during the spring (March to June) when it can have the most pronounced impact peatland hydrological function, is largely unknown.

WBP peatlands are under pressure from resource extraction in the Athabasca Oil Sands Region, where they are removed during surface mining processes or impacted during other development activities (Rooney, Bayley, & Schindler, 2012), and from climate change (Ireson et al., 2015; Waddington et al., 2015), both of which can alter or remove peatlands, removing a water source from the landscape. Climate change predictions for the WBP suggest warmer air temperatures particularly in the winter months (Jiang, Gan, Xie, Wang, & Kuo, 2017) and an increase in the length of the snow-free season (Vaughan, Comiso, Allison, Carrasco, Kaser, et al., 2013). Precipitation is projected to increase (Mbogga, Wang, & Hamann, 2010; Wang, Hogg, Price, Edwards, & Williamson, 2014); however, there is uncertainty if this is enough to offset higher evaporative losses (Ireson et al., 2015; Thompson, Mendoza, & Devito, 2017). Thus, understanding the potential impacts of SGI on the ecohydrology of peatlands in the WBP and Athabasca Oil Sands Region is important for reclamation work and to understand how these systems may respond to climatic change.

Therefore, the goal of this paper is to evaluate the potential role of concrete SGI (herein referred to as SGI) during the spring melt in a WBP peatland, determining whether the net effect is to enhance or diminish water losses via evapotranspiration. The objectives are to (a) quantify SGI characteristics during the melt period and determine the influence of microtopography on ice structure and melt rate; and (b) determine the relationship between SGI and hydrological processes (i.e., water table depth, soil moisture, PET, and AET) to better understand the SGI role in WBP peatland ecohydrology.

2 | STUDY AREA AND METHODS

A field study was completed from April 7 to June 26, 2017, at Pauciflora Fen, a poor fen (56°22'30.36"N, 111°14'3.29"W) approximately 40 km south of Fort McMurray, Alberta (Figure 1a,b). Pauciflora Fen is located on the Stoney Mountain complex within the WBP, where a subhumid climate is present. The 30-year climate normal for the area shows a mean annual temperature of 1.1°C and a mean rainfall of 307 mm (Fort McMurray Airport, Environment Canada), whereas mean snow water equivalent (SWE) is

approximately 104 mm, calculated from an empirical relationship between air temperature and snow density (Hedstrom & Pomeroy, 1998). However, Pauciflora has a wetter climate compared with typical peatlands in the WBP due to its higher elevation in the Stoney Mountains, with a 6-month growing season (April to September) mean over 4 years (2011–2014) precipitation of 412 mm due to orographic precipitation (Wells, Ketcheson, & Price, 2017), approximately 100 mm higher compared with the 30-year climate normal. The 4-year mean exceeds the mean PET (369 mm) during the growing season, indicating that Pauciflora may not be subject to the same subhumid climate as frequently as other peatlands in the surrounding area.

The fen has an area of 0.11 km² and is bounded by a road to the north, where a culvert (Figure 1c) acts as an outlet, and by forested hillslopes surrounding the rest of the fen. Field data were collected in a sparsely treed area of the fen (peat thicknesses ≈ 4 m) corresponding with the "neck," part of the North Fen in Wells et al. (2017). The entire fen is underlain primarily by fine-grained silt with a high clay fraction (Wells et al., 2017). Trees were composed of *Picea mariana* and *Larix laricina* (Figure 1d,e), located between two hillslopes on the east and west sides of the fen. Understory vegetation is composed of a carpet of *Sphagnum* moss. A detailed description of the fen vegetation can be found in Bocking, Cooper, and Price (2017) and the hydrogeological setting in Wells et al. (2017).

2.1 | Micrometeorological variables

Air temperature (°C), relative humidity (%), windspeed (m/s), and net radiation (W/m²) were measured at a 60-s interval using a CR1000 data logger (Campbell Scientific Ltd., Logan, Utah) and averaged at 30-min intervals. Air temperature and relative humidity were measured 2 m above the surface (HMP35C, Vaisala, Helsinki, Finland). Wind speed and direction (RM Young 05103, Campbell Scientific, Logan, Utah) and net radiation (CNR4 Net Radiometers, Kipp & Zonen, Delft, Netherlands) were measured at 6 m. Precipitation was measured on site, approximately 200 m north of the met station using a tipping bucket rain gauge (HOBO Onset, Hoskins Scientific, Burlington, Canada) connected to a CR1000 Campbell Scientific datalogger.

AET was measured continuously and recorded at half hour intervals, 4 m above the ground surface using an eddy covariance (EC) system, and summed to daily values, following similar approaches used in boreal peatlands (Brown et al., 2010; Warren et al., 2018; Wells et al., 2017). The EC system consisted of a 3D sonic anemometer (Gill Windmaster Pro, Gill Instruments, Lymington, UK) and a closed-path infrared gas (CO₂/H₂O) analyser (LI-7200, LICOR Inc., Lincoln, Nebraska) sampled at 20 Hz. EC data were processed in EddyPro software (LI-COR Inc., Lincoln, Nebraska, USA), in which corrections were made for time lag and sensor separation (Fan, Wofsy, Bakwin, Jacob, & Fitzjarrald, 1990), coordinate rotation (Kaimal & Finnigan, 1994), periods of low turbulence and energy balance closure (Petrone, Chasmer, Hopkinson, Silins, Landhausser et al., 2014), and density effects (Burba et al., 2012). A footprint analysis (Kljun, Calanca, Rotach, & Schmid, 2004) was completed in order to remove any fluxes

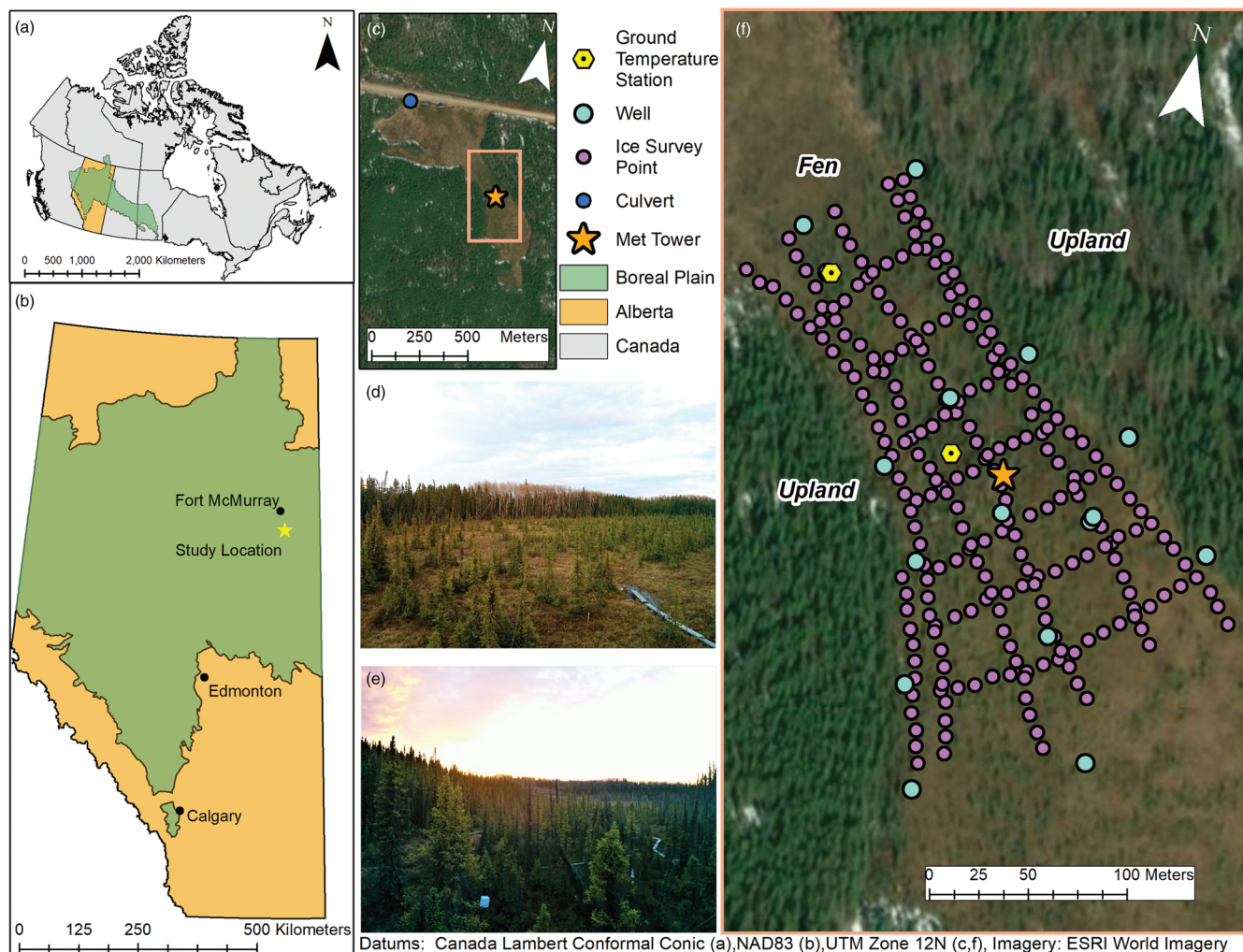


FIGURE 1 (a) The location of Alberta within Canada. (b) The location of Pauciflora within Alberta and the Boreal Plain. (c) The location of the culvert (outflow) relative to the survey area (d) looking south from the met tower showing the canopy characteristics of the site, (e) looking north showing the proximity of the west hillslope and the mid fen temperature ground station (white box near the bottom of the image). (f) Map shows the study area within Pauciflora Fen including the well monitoring network, placement of ground temperature monitoring stations, and the ice survey

from the flux total that were found to originate outside of the fen. The mean flux footprint (2014–2018) area was 0.0032 km², extending \approx 41 m north, \approx 37 m south, \approx 26 m west, and \approx 22 m east from the EC system.

2.2 | Ice and snow surveys

Ice surveys were conducted on April 8, 10, and 13, May 3, 9, 16, 23, and 30, and June 6, 2017, nine in total. The spatial extent, and depth to SGI, was determined using 13 transects with survey points spaced 5 m apart within each transect (Figure 1f). Four measurements of depth to SGI were taken within 1 m of the survey point by inserting a graduated steel rod into the peat until resistance was met. This method has been reported to have an error up to 4 cm in fen peatlands (Woo & Xia, 1996) due to peat compaction from the sampler's weight but was deemed acceptable because it allowed for

broad spatial measurements. At every second survey point, volumetric moisture content (VMC) in the near surface (0- to 5-cm layer) was measured in triplicate and averaged, using a WET-2 soil water sensor (Delta-T Devices, Cambridge, UK), using organic soil parameters as defined by the moisture metre. The 0- to 5-cm layer coincides with the living *Sphagnum* moss layer in the peat profile and contains the capitulum, the site of photosynthesis in *Sphagnum* mosses (Schipperges & Rydin, 1998). Low VMC in the 0- to 5-cm layer can be an indicator of moisture stress for the mosses.

Two hundred forty survey points were measured and classified based on observation of microtopographical form. Hollows were localized depressions where the water table was often visible, hummocks were visibly raised mounds, and lawns were within larger flat areas with no visible hummock-hollow topography. A dual-frequency survey-grade differential global positioning system (Topcon GMS-2, 2011–2012; Leica Viva GS14, 2014) quantified the longitude, latitude,

and absolute elevation of each survey point and well location (vertical accuracy ± 0.5 cm).

Four snow surveys were carried out on April 18, 21, 25, and 29 following snow events on April 16 and 17, prior to these dates, the site was snow free. Snow depth was measured along a transect that ran from north to south through the ice survey area using a standard Meteorological Service of Canada snow tube sampler. In order to calculate SWE, snow pits were dug near the transects to obtain representative values of snow density using standard methods (Adams & Barr, 1974). The average SWE for the ice survey area was calculated by multiplying the average density by the average depth for each snow survey.

2.3 | Water table dynamics

Water table was measured manually with a blowstick using 14 monitoring wells constructed from polyvinylchloride (2.5-cm inner diameter) pipe and screened with 2" glass fibre-based well sheathing well sock (Rice Engineering, Edmonton, Alberta). Wells were installed to a depth of 1 m below the ground surface. Pre-existing wells within the fen, labelled with the prefix "T2" in Wells et al. (2017), were also used. Due to differences in sampling location of the SGI and water table depth, interpolated surfaces of the water table were created using an inverse distance weighting (IDW) method in ArcGIS 10.1 with a 1-m cell size and a fixed distance search radius of 12 m. The SGI survey was overlain onto the water table surface, and each survey point compared with the underlying water table cell value. Water table and depth to SGI were compared on May 3, 9, 16, and 23 spanning the majority of the melt period. Note that for May 16 and May 23, the water table data are taken from May 17 and May 22, respectively.

2.4 | Peat ground temperatures and impacts on available energy

Peat subsurface temperatures were recorded at two locations, the mid fen (MF) located 11m north-west of the met tower, had a more open canopy compared with the north treed fen (NTF; Figure 1d,e) located 70 m north of the met tower. For each location, two wooden stakes had eight holes drilled into it that corresponded with the measurement depths (MF: 2, 5, 10, 20, 50, 75, 100, and 150 cm; NTF: 2, 5, 10, 20, 30, 40, 50, and 60 cm). Type-T thermocouple (Omega Engineering, Norwalk, Connecticut, USA) was inserted into each so that just the exposed metal tips of the wire were extended past the wood. Each wire was sealed using an epoxy resin. One stake was inserted into a hummock and the other into an adjacent hollow and each thermocouple wired into a Campbell Scientific logger (CR1000 Campbell Scientific Ltd., Logan, Utah). These data were used to determine temperature gradients for the 2- to 5-cm peat soil layer, where negative temperature gradients indicate that the peat surface is warmer than deeper soil layers. A temperature gradient of 0 represents isothermal conditions in the top 5cm of the peatsoil.

The relationship between the spring ground heat flux (Q_G), SGI, and PET was assessed for each spring from 2013 to 2018.

Calorimetric Q_G was calculated using the full temperature profile from the MF ground temperature station following the approach of Halliwell and Rouse (1987). Calorimetric Q_G was used in the Penman-Monteith equation (Monteith, 1965) to calculate three daily PET rates for the duration of each ice melt period from 2013 to 2017: (a) considering the calorimetric Q_G ($PETQ_{G_{cal}}$), (b) ignoring Q_G ($PETQ_{G_{none}}$), and (c) assuming Q_G is equal to 10% of net radiation ($PETQ_{G_{10}}$). Only PET daily values that coincided with SGI melt were used for comparisons. PET for this study corresponds to wet-surface evapotranspiration, which considers available energy and atmospheric conditions, and as such represents an upper limit of PET (Granger, 1989). The relationship between AET and depth to SGI was evaluated by comparing AET measured by the EC system to the depth of the 0-degree isotherm (assumed to equal the depth to SGI) and the 2- to 5-cm temperature gradient measured at the MF ground temperature station. Due to a lack of data overlap between the EC system and when SGI was present at the ground temperature monitoring station, only the data from the spring of 2015 and 2018 were used. Both of these springs were warmer and had thinner SGI based off of the ground temperature profiles. As a result, the melt periods (9 days for 2015 and 3 days for 2018) were much shorter compared with the 2017 melt period (19 days).

2.5 | Spatial interpolation

An IDW was used to spatially interpolate each survey with a cell size of 1 m. Ice-free areas were included in the IDW process by creating Thiessen (1911) polygons around each ice-free survey point and added as breaklines in the IDW. A summary of the survey points and cross validation results are shown in Table 1. The volume of ice that melted from above for each cell can be calculated using the following equation:

$$V_{ice} = ((\Delta Z_{ice} \times \text{Surface Area}) \times \Phi), \quad (1)$$

where V_{ice} is the volume of ice (m^3) for each cell, ΔZ_{ice} is the change in ice elevation, surface area is the cell raster size ($1m^2$), and Φ is the total porosity. An IWE depth (mm) was calculated using

$$IWE = \left(\frac{[V_{ice} \times VExp_{ice}]}{[\text{Surface Area}]} \right) \times 1,000, \quad (2)$$

where IWE is the ice water equivalent (mm) and $VExp_{ice}$ is the volume expansion of ice (9%). In an effort to better ascertain the error associated with peat compaction, ice measurements were made with a frost probe at the MF and NTF ground temperature stations in 2018. The average difference between the measured ice and the interpolated 0-degree isotherm was $-3cm$ (25mm in IWE) for the MF and $-1.4cm$ (12mm in IWE) for the NTF, which is below the estimated error values due to compaction reported by Woo and Xia (1996) and support the confidence in IWE reported below.

TABLE 1 Cross validation results for the inverse distance weighted interpolations for the ice and water table surveys

Survey date	RMSE (cm)	Mean error (cm)	Sample size
Ice survey			
May 3, 2017	0.063	0.00048	240
May 9, 2017	0.079	0.0013	207
May 16, 2017	0.10	0.0014	177
May 23, 2017	0.12	0.0024	138
June 6, 2017	0.13	-0.0030	25
Water table survey			
May 3, 2017	4.2	0.2	11
May 9, 2017	5.9	0.26	12
May 16, 2017	3.7	0.69	12
May 23, 2017	9.3	2.8	14
June 6, 2017	11.8	4.3	15

Note. RMSE is the root mean square error.

2.6 | Peat hydrophysical properties

Twelve unfrozen cores approximately 40 cm in length were taken from hummocks ($n = 6$) and hollows ($n = 6$). Hummock cores were taken by inserting polyvinylchloride pipe into the moss and cutting through the moss on the outside of the pipe with a hand saw. Hollow cores were taken using Wardenaar Peat profile sampler (Eijkelkamp, The Netherlands). Cores were wrapped in plastic wrap, frozen, and then transferred to the Hydrometology Lab, University of Waterloo, where peat porosity and bulk density were determined using methods outlined by Boelter (1969).

3 | RESULTS

3.1 | Ice melt and IWE

Pauciflora was found to be snow free on April 8, and three SGI surveys were completed on April 8, 10, and 13. SGI was <30 cm below the surface, and no significant differences (pairwise Wilcoxon test) were noted in ice depth between the three survey days ($p \leq .05$) indicating that minimal melting occurred over this period. Two snow events (total SWE ≈ 64 mm) on April 16 and 17 delayed any further ice surveys until snow free conditions on May 1. Six ice surveys were completed in May and June, each differing significantly from each other in depth to ice ($p \leq .01$; Figure 2). Results from the surveys show a gradual melt over the month of May and into the month of June. From May 3 to May 23, median depth to ice increased from 8.8 to 32.3 cm while 102 survey points became ice free over a 20-day span (Figure 2). From May 23 to June 6, the median depth to ice increased to 57 cm, coinciding with an additional 113 survey points becoming ice free but was over a 15-day span. By June 6, the SGI was quite deep and sporadic, and the majority of the survey area was ice free.

Depth to SGI differed significantly within each microtopographic form between ice surveys, where all p values for each microtopographic form were <.01 (pairwise Wilcoxon). However, the daily average melt rate between microforms did not differ significantly during the month of May (Figure 3). Daily median melt rate ranged from 0.05 to 1.2 cm/day (Figure 3). The lowest melt rates occurred between April 13 and May 3, where the fen was covered in snow until May 1. Beginning in May, daily median melt rates were fairly consistent, ranging from 0.5 to 1.2 cm/day. Melt rates for all microforms for the May 3–9 and May 16–23 ice surveys were higher compared with May 9–16 (Figure 3), which coincided with cooler air temperatures and a snow event on May 14. All three microforms

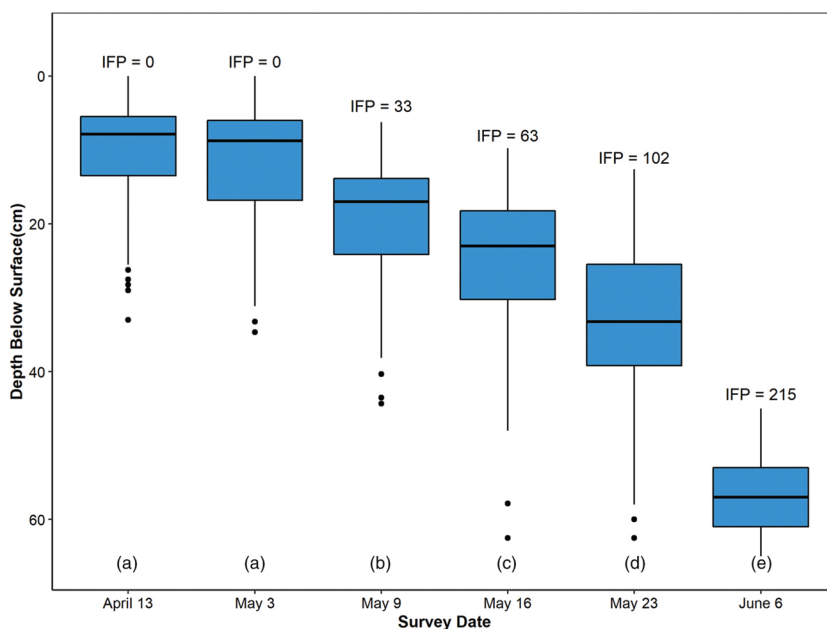


FIGURE 2 Ice depths for ice surveys completed on April 13, May 3, May 9, May 16, May 23, and June 6 with the number of ice free points (IFP) for each survey. Different letters indicate statistically significant differences (pairwise Wilcoxon, $p < .05$). The ice survey on May 30 was removed due to insufficient data

FIGURE 3 Daily average melt rate between ice survey dates, grouped by microtopography, where avg melt rate = Difference in ice depth/ number of days between surveys. Different letters indicate statistically significant differences (pairwise Wilcoxon, $p < .05$) within each group

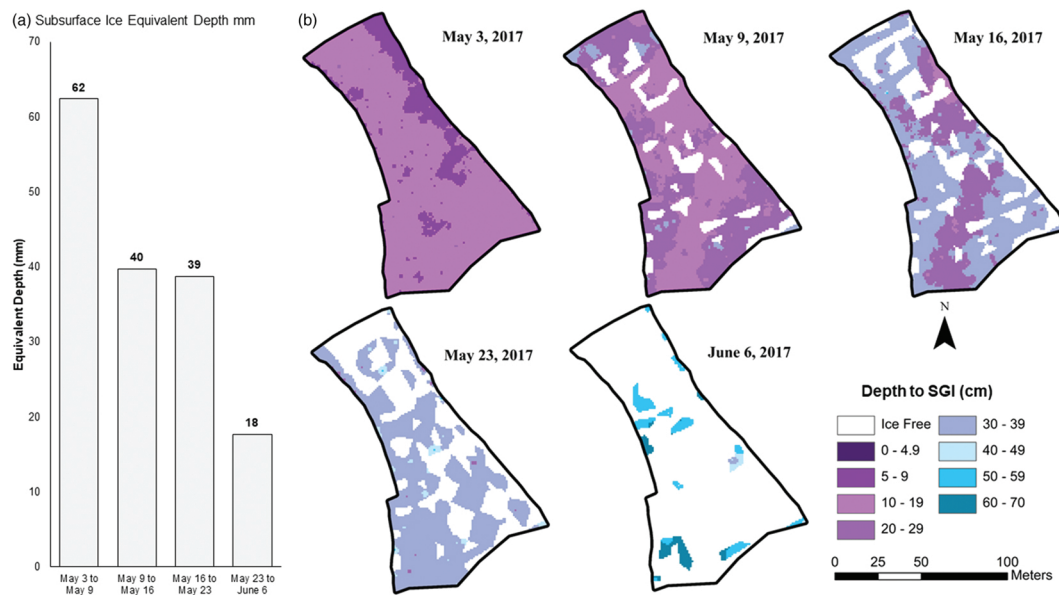
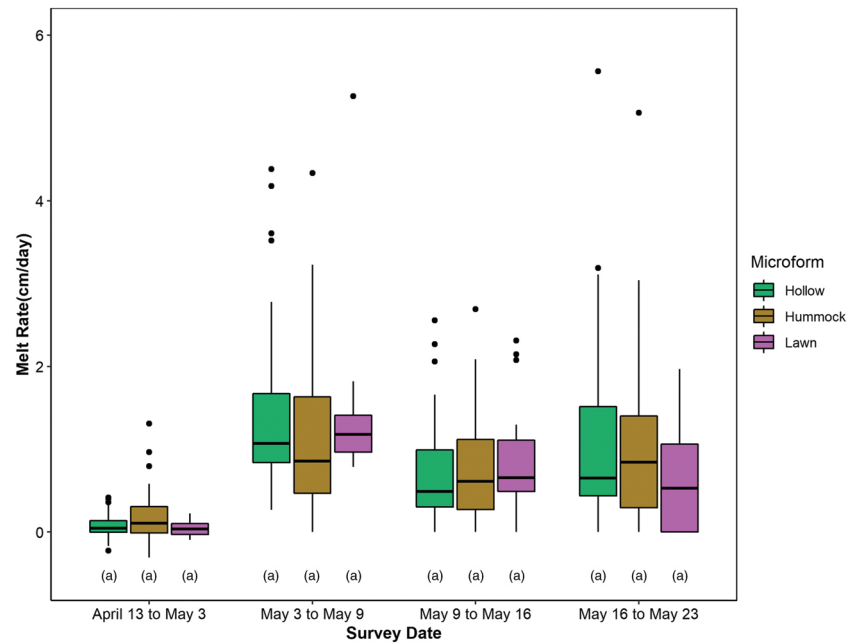


FIGURE 4 (a) The ice water equivalent released between each ice survey (b) maps showing the depth to SGI on each survey day

exhibited higher melt rates earlier in the season (see May 3–9) compared with the rest of the month. Lawns initially thawed faster than hummocks and hollows. However, during the mid and late portions of the month, hummocks and lawns thawed slightly faster than hollows. The May 23 to June 6 melt rates were not included due to low sample size. The amount of water released from the top of SGI during melting (Figure 4) was calculated for each melt period using Equations (1) and (2), the SGI IDW surfaces, and an average porosity of 0.97, based on the peat core hydrophysical properties (Table 2). A melt period was defined as the difference between two consecutive SGI surveys. Mean ice depth (+SD) below the peatland surface on May 3 was 12 cm (+2 cm) and increased to 20 cm (+3 cm) on May 9. This

coincided with the highest melt rate and produced approximately 62 mm of IWE, the highest release of water for the spring. This IWE was slightly lower than the combined total (80 mm) of rain (16 mm total, April to May) and end of winter SWE (SWE = 64 mm, data not shown) released during snowmelt at the end of April following the major snow event on April 16. Subsequent IWE was lower, coinciding with an increase in the number of measured ice-free survey points, and a decrease in the melt rate. A decrease in melting due to a snow event on May 14 also contributed to slower melt rates, reducing the IWE later in the melt period.

Using the mean ice depths for each survey date permitted an approximation of the depth where the water was being released.

TABLE 2 Average porosity and average bulk density from peat cores

Core	Depth interval (cm)	Porosity	Porosity standard deviation	Bulk density	Bulk density standard deviation	No. of samples
T2 center (hummock)	0–40	0.98	0.01	0.04	0.01	8
T2 center (hollow)	0–40	0.98	0.01	0.04	0.01	4
T2 east (hummock)	0–40	0.97	0.01	0.05	0.02	7
T2 east (hollow)	0–30	0.95	0.03	0.08	0.04	3
T2 west (hummock)	0–40	0.96	0.01	0.06	0.02	5
T2 west (hollow)	0–60	0.96	0.03	0.07	0.04	6
Average of all samples	—	0.97	0.02	0.05	0.03	33

Note. Averages are determined from the individual porosity and bulk density values at 5-cm depth intervals (hummocks) and 10-cm depth intervals (hollows).

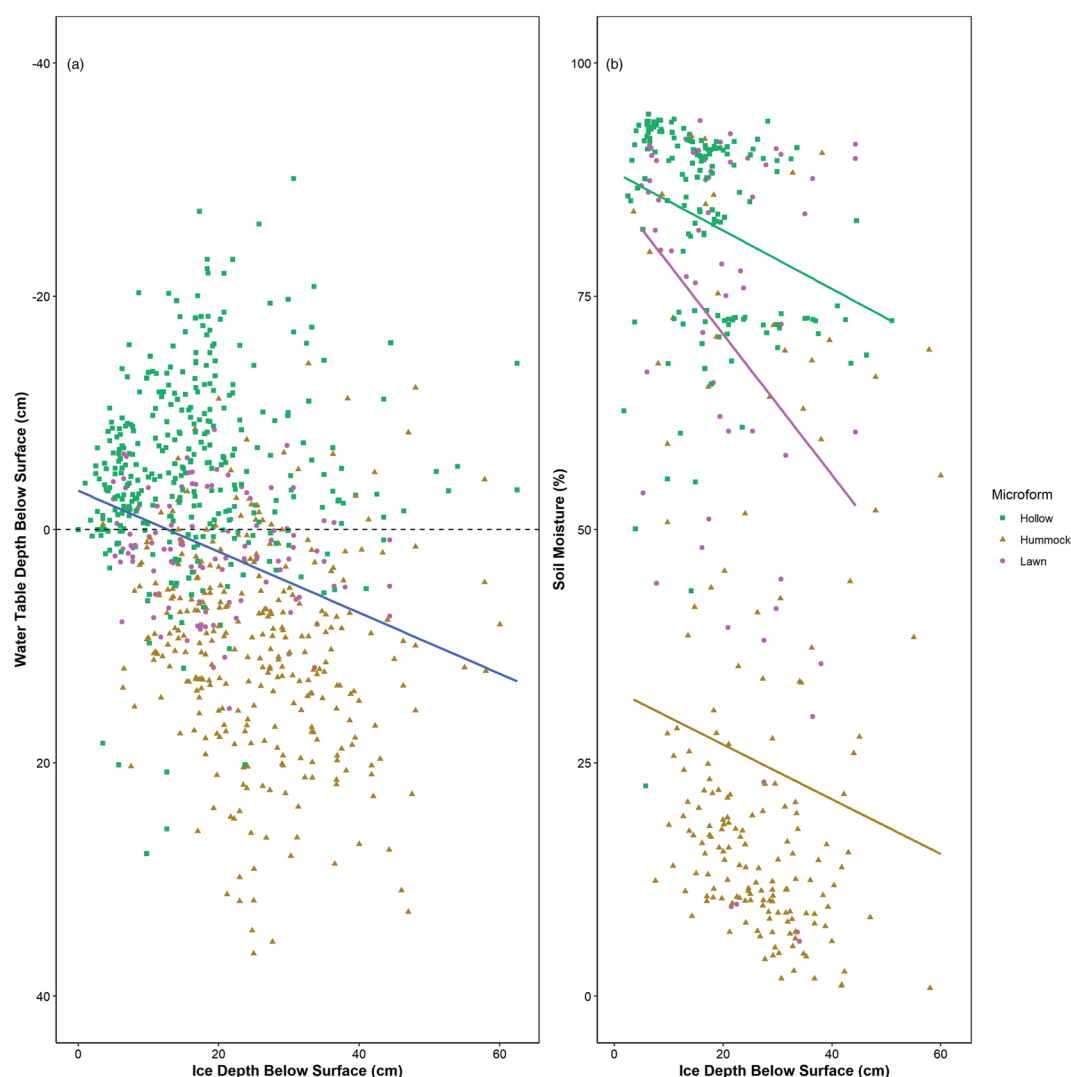


FIGURE 5 (a) The relationship between ice depth and water table. A significant negative relationship was found (Kendall tau = -0.21 , $p < .01$); 0 indicates the peatland surface, where a negative value is above the surface and a positive value is below the surface. (b) The relationship between ice depth and soil moisture (0–5 cm). Significant negative relationships were found for all microtopographic forms (hummock Kendall tau = -0.22 , $p < .01$; hollow Kendall tau = 0.30 , $p < .01$; lawn Kendall tau = -0.22 , $p < .05$)

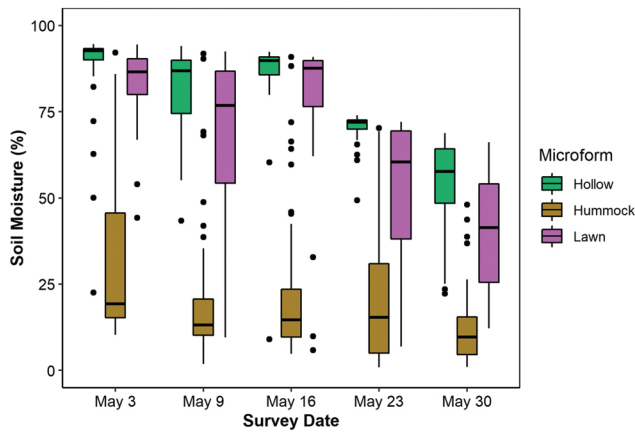


FIGURE 6 Soil moisture (0–5 cm) measurements grouped by microtopography for each ice surveyday

Approximately 89% or 141 mm of IWE (Figure 4a) was available in the top 33 cm of the peat profile (Figure 4b). The remaining 11% equated to 18 mm from May 23 to June 6.

3.2 | SGI, water table, and soil moisture

For the 2017 study period, the water table was consistently above the upper boundary of the SGI. The relationship between water table and SGI is shown to have a significant negative linear relationship (Kendall tau = -0.21 , $p < .01$; Figure 5a), where shallower ice depths are associated with greater water table depths. When grouped by microtopographic form, water table depth and SGI exhibited a weak significant relationship (hummock Kendall tau = -0.13 , $p < .01$; hollow Kendall tau = 0.09 , $p < .05$; lawn Kendall tau = -0.14 , $p < .05$). The water table showed a small decline in mean depth below ground surface from May 3 ($3.4 \text{ cm} \pm 8.8 \text{ cm}$) to May 23 ($6 \text{ cm} \pm 9.2 \text{ cm}$). Due to the snow event on May 14, the median water table rose to 3.3 cm above the ground surface on May 16. The VMC (top 5 cm) was relatively high across all three microforms on May 3 with median values of 92.7%, 86.5%, and 19.3% for hollows, lawns, and hummocks,

respectively, but decreased with time (Figure 6). By May 30, soil moisture had dropped significantly relative to initial measurements for hollows (57.7%), lawns (41.4%), and hummocks (9.7%; pairwise Wilcox, $p < .01$). The decline in VMC occurred along a microtopographical gradient, with hummocks being the driest (median range 9.7–17.8%) and hollows the wettest (median range 57.7–92.7%). The decline with VMC over May declined with an increasing depth to SGI (Kendall tau = -0.36 , $p < .01$). When grouped by microtopographic forms (Figure 5b), there were significant negative relationships between SGI and VMC (hummock Kendall tau = -0.22 , $p < .01$; hollow Kendall tau = 0.30 , $p < .01$; lawn Kendall tau = -0.22 , $p < .05$).

3.3 | SGI, AET, PET, and ground heat flux

SGI began melting in April for 2015 and 2018, where the 2015 melt period totalled 7 days whereas the 2018 melt period totalled 3 days (Figure 7b). For both 2015 and 2018, depth to SGI and melt rate did not exhibit any significant relationships with daily AET in 2015 or 2018 (data not shown). However, there is a shift in the variability of daily AET that coincides with negative temperature gradients between 2 and 5 cm below ground surface (Figure 7a). Under such conditions, daily AET varied considerably (mean = 1.3 mm/day , $SD \pm 0.81 \text{ mm/day}$, $n = 26$), but once the ice began to melt, the variability decreased (mean = 1.8 mm/day , $SD \pm 0.36 \text{ mm/day}$, $n = 16$), and daily AET rates were between 2 and 3 mm/day. The transition from isothermal to negative temperature gradients coincided with the beginning of ice melt for 2015 and 2018 (Figure 7b). The cumulative PET rates calculated for ground heat flux method for each year are shown in Figure 8. When including Q_L , Q_G is increased thereby reducing the available energy for PET. Figure 8 shows an average 10-mm reduction when compared with $PET_{Q_{none}}$ and an average 6-mm reduction when compared with $PET_{Q_{10}}$ while ice is melting. The largest reductions in PET coincided with cooler air temperatures during the spring, such as 2014 and 2017, which also had longer melt periods (data not shown). In 2015 and 2016, when the spring was warmer, $PET_{Q_{cal}}$ was slightly lower. These springs also experienced shorter

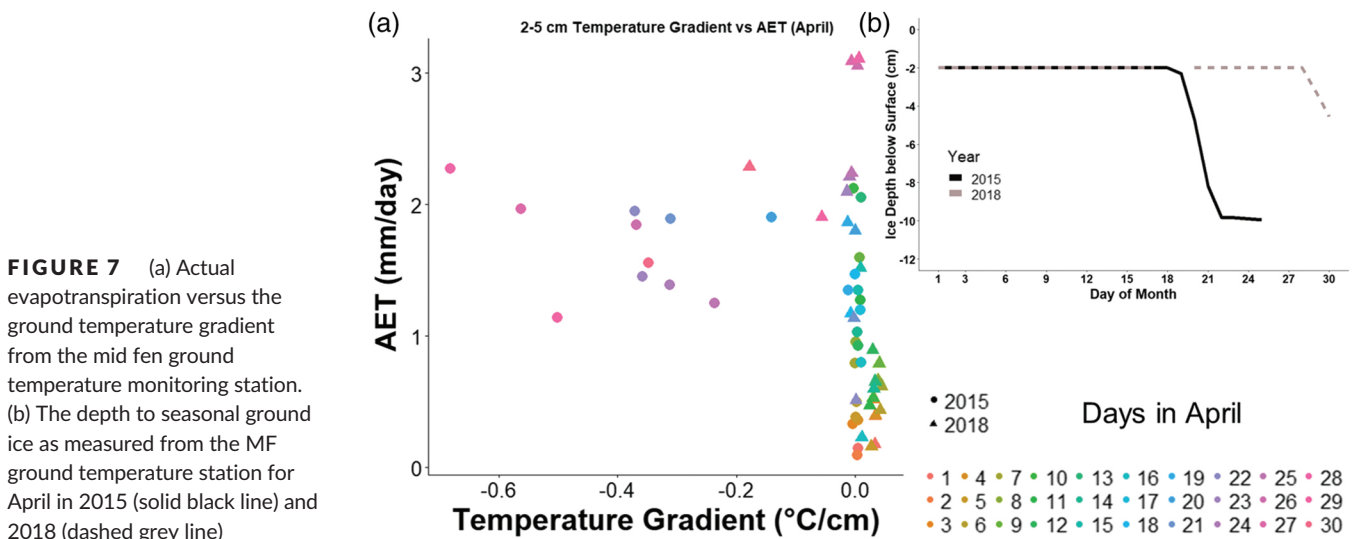


FIGURE 7 (a) Actual evapotranspiration versus the ground temperature gradient from the mid fen ground temperature monitoring station. (b) The depth to seasonal ground ice as measured from the MF ground temperature station for April in 2015 (solid black line) and 2018 (dashed grey line)

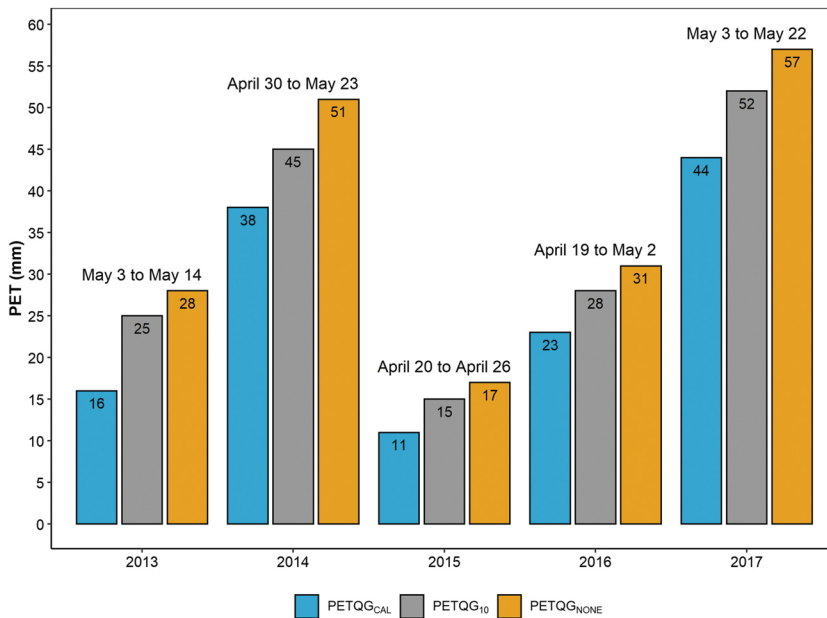


FIGURE 8 The reduction in potential evapotranspiration using three different ground heat flux approaches, the calorimetric method (PETQG_{CAL}), assuming QG is equal to 10% of net radiation (PETQG₁₀), and not including the ground heat flux (PETQG_{NONE}). The melt period and time the model was run for are stated above each year

melt periods, with SGI free conditions occurring at the beginning of May (data not shown).

4 | DISCUSSION

4.1 | Ice melt and IWE

In 2017, Pauciflora became SGI free approximately 1–2 months earlier than what was reported for other WBP spruce peatlands (Brown et al., 2010; Petrone, Devito, Silins, Mendoza, et al., 2008; Thompson & Waddington, 2013). Pauciflora exchanges ground water with adjacent hill slopes (Wells et al., 2017), which means it is possible that bidirectional melting is reducing the time required for the peatland to become SGI free (FitzGibbon, 1981). Similar timing of SGI free conditions were reported by Smerdon and Mendoza (2010) in a riparian peatland by the end of April, attributed to water exchanges with an adjacent lake. A 3-year study by Elmes, Thompson, Sherwood, and Price (2018) on a rich fen reported SGI free conditions, which ranged from late April to mid-May, which they attribute to low water tables prior to freezing, which prevented the formation of concrete SGI. The faster melting at Pauciflora was not expected due to the cooler climate compared with other WBP peatlands. Wetter surface conditions at Pauciflora may also have increased melt rates. The presence of water on ice enhances melting (Wright, Hayashi, & Quinton, 2009) due to its higher thermal conductivity relative to air (Todd, 1909). For Pauciflora, the elevated soil moisture in the upper 2–5 cm (Figure 6) may have offset the effects of its generally cooler climate.

The lack of significant differences in melt rate between each microform (Figure 3) is likely due to difference in the structure of the SGI (i.e., concrete vs. reticulate), thermal characteristics of the peat, and the methodologies employed. Only the melt rates of concrete SGI were considered, which does not capture the faster melting of reticulate SGI. The concrete SGI measured in the hummocks begins at

approximately 30 cm below the ground surface. The lower thermal conductivity of thawed unsaturated peat (Farouki, 1981; Woo & Xia, 1996) and its ability to reduce ice melt (Jones, Castonguay, Nasr, Ogilvie, & Arp, 2014) insulated the SGI under hummocks and slowed melting. This is indicated by the higher melt rates in hollows and lawns compared with hummocks during the first week of melt (Figure 3). The slightly higher rates in hollows and lawns are likely due to melt-water collecting in lower lying areas at the surface, which can preferentially melt the ice (Hayashi et al., 2007). This can create a positive feedback where depressions form in the SGI where subsurface water can collect, further enhancing melt (Wright et al., 2009). However, as SGI continued to melt, there were no further differences between microtopographic forms' melt rate.

These negligible differences suggest that SGI does not have to melt beyond 5 cm below the hollow surface before differences in melt rate are reduced by the thermal properties of the peat overlying the SGI. Although unfrozen VMC at the base of hummocks was not directly measured, the relatively close proximity of the water table (Figure 5a) near the hummock base implies a high unfrozen VMC, likely similar to hollows and lawns. Additionally, ponded water over a hollow could move laterally into a hummock, providing additional thermal energy to melt SGI beneath the hummock. This could create similar thermal conditions between the base of the hummocks, hollows, and lawns, reducing melt rate variability. The transect point spacing (5m) within each transect may also impact the results. If a smaller spacing (≤ 1 m) was used, it is possible that different microforms closer to each other may exhibit different melt rates. However, at basin scale, these trends were not evident, which suggests that at a larger scale, the influences of microtopography on melt are negligible for Pauciflora.

As SGI melted, a considerable amount of liquid water (≈ 159 mm) was released in the near surface layers of the peat moss, of which 141 mm was released in the upper 30cm of the peat soil. The limited

amount of water received via snowmelt ($SWE \approx 64$ mm) and measurable rain (16 mm) during April and May of 2017 highlights the importance of this water from melting ice, particularly under the dry conditions typical in the WBP. While a long-term P record for Pauciflora does not exist, Wells et al. (2017) completed a 4-year study from 2011 to 2014 and found that the average P input for April and May is 69 mm, which was below PET (79 mm). This indicates that the release of melt water is important during the spring even for a wetter site such as Pauciflora. The impact of SGI may be larger for surface vegetation in drier peatland systems in the WBP. At a site with similar surface vegetation in the Alaskan Boreal forest, Young-Robertson, Ogle, and Welker (2017) have shown that vascular plants will tap into ice water under dry conditions. For *Sphagnum* mosses, which do not have root systems to tap into deeper water, wet conditions in part maintained by the SGI may provide optimal moisture conditions for mosses to begin photosynthesizing (Moore et al., 2006), which could increase moss resiliency to stress.

4.2 | SGI-water table and near surface VMC

Although the high relative position of SGI likely promoted a high water table by blocking snowmelt from infiltrating (Ireson et al., 2015), only weak correlations were evident in the three microtopographic forms (Figure 5a) with hummocks and lawns exhibiting a weak negative relationship, whereas hollows had a weak positive relationship. This difference in relationship sign between microforms is likely due to the snow event that occurred on May 14 and the subsequent snow melt over the next 48 hr, where hollows may have shown a more prominent response in water table depth. As SGI free areas opened up, liquid water released from melting SGI would help offset the impact of water table drawdown from evaporation. Figure 5a shows that for all microtopographic forms, the water table was often within 20 cm of the surface (the 0 mark on the y-axis) for the duration of the ice surveys. The gradual increase in SGI free conditions with minimum change in water table depth suggests that the spatial continuity of SGI does not control the water table depth at Pauciflora during the spring. This could be because the water table depth is usually within 20 cm of the surface (Wells et al., 2017). However, if the lower boundary of the SGI and the water table depth is decoupled over winter forming an unsaturated zone beneath a SGI layer, it is possible that spatial discontinuities in SGI may be more important. Elmes et al. (2018) reported over-winter water table drawdown, whereas a frozen reticulate ice layer persisted in the top 20 cm of the peat. Although Wells et al. (2017) reported a water table increase over the winter at Pauciflora in 2011, it is possible that SGI could separate from the water table via other mechanisms due to frost heave (Kingsbury & Moore, 1987), moisture migration towards the freezing front (Cheng & Chamberlain, 1988; Talamucci, 2003), or if any outflow from the fen occurs after SGI formation. Decoupling of a frozen peat layer and the water table below has been reported before (Kingsbury & Moore, 1987). Rather quick water table drawdown was observed in the 2018 spring at Pauciflora where a change in surface ponding water of approximately 5 cm was noted relative to black spruce trunks over

3 days. However, thawing of any ice dam in the culvert may also explain the observed decrease in ponded water, by allowing for more rapid discharge from the fen. Further evidence is needed though to confirm whether the drawdown was due to a decoupled water table or the ice dam thawing in the culvert.

It was hypothesized that there would be a relationship between depth to SGI and VMC. Melting SGI close to the peatland surface would act as a close supply of water for the surface vegetation. As the depth to SGI increased, VMC decreased. However, the weak (Kendall $\tau = -0.36$), significant ($p < .01$) relationship between SGI position and VMC (0–5 cm) appears to suggest minimal influence. There are several reasons why this may be.

First, the mean porosity of the moss and peat (0–40 cm) in hummocks (mean porosity = 0.97 ± 0.01 , $n = 20$) and hollows (mean porosity = 0.96 ± 0.02 , $n = 13$), which is typical of peatlands in the WBP (Goetz & Price, 2015; Petrone, Devito, Silins, Mendoza, et al., 2008; Redding & Devito, 2005), indicate large pores near the surface. Larger pores facilitate larger changes in VMC with relatively small increases in water table depth (Waddington et al., 2015) because larger pores will drain before smaller pores. For the upper layers of the moss, this may mean that there is no gradual decline in VMC with ice depth but rather a step change in soil moisture. Such a change is evident with hollows, where a clear drop from approximately 90% to 75% is evident (Figure 5b). However, this step change is not evident for hummocks and may be due to the VMC sampling location at the top of the hummock, where a larger step change in VMC may not be captured. An associated shift along the x-axis indicated that the drop may be a result of increasing depth to SGI, which also coincided with an increasing water table depth.

The generally weak relationships (Kendall $\tau < 0.3$) for each microtopographic form may also be due to the site location. Pauciflora is a wet site (Wells et al., 2017) compared with other peatlands in the area (Elmes et al., 2018; Wells & Price, 2015), and the potential range of soil moisture during spring conditions was likely not captured in 2017 explaining the weaker relationships found between SGI and VMC. Further study is needed to assess this relationship under dry and wet spring conditions. Depth to SGI, water table depth, and VMC exhibited a general decline over May (Figures 2, 5, and 6), suggesting such relationships could be masked by the generally wetter conditions. Figure 5a shows that there is a significant relationship between SGI and water table depth at Pauciflora. Using microtopography as a proxy for variable SGI and water table depth, increasing depth to SGI is associated with generally drier conditions. This supports the hypothesis that melting SGI closer to the surface may indeed promote wetter conditions. The sharp drop in hollow VMC with increasing depth to SGI suggests that the impact of SGI on VMC may vary with microtopography.

4.3 | SGI and evapotranspiration

There is a clear distinction between the soil temperature gradient and AET (Figure 7a) under isothermal conditions and when the ice is melting. AET ranges from 0 to 3 mm/day, but as the temperature gradient

becomes negative (i.e., ice melt), AET becomes constrained to 1.5–2.5 mm/day. The reduction in range of AET coincides with the beginning of ice melt in 2015 and 2018. This is indicative of the larger Q_{GL} component of Q_G being considered and is caused by the ice phase change to water (Hayashi et al., 2007; Woo & Xia, 1996), increasing Q_G and reducing available energy. Although these results support the findings of Petrone, Devito, Silins, Mendoza, et al. (2008) that the presence of melting SGI promotes AET, they also indicate that the melting SGI holds AET rates relatively constant. The reduced variability may lead to an overall reduction in AET, which may help keep WBP peatlands wet during drier springs. The overall impact of this potential influence will depend on the persistence of SGI. Also, it is possible that this effect could be reduced by lateral melting induced by ground water inputs as the SGI becomes spatially discontinuous. This means that the energy required for melting the ice is not being supplied entirely at the surface via conducted solar energy. To what extent this is occurring though is unknown and requires further study.

Increases in Q_{GL} due to melting SGI also resulted in a reduction in PET across all 5 years when compared with $Q_G = PETQ_{G10}$ or $Q_G = PETQ_{G_{NONE}}$ (Figure 8). The average difference between $PETQ_{G10}$ and $PETQ_{G_{CAL}}$, and $PETQ_{G_{NONE}}$ and $PETQ_{G_{CAL}}$ was small, averaging 6 and 10 mm, respectively. Over the typical melt period at Pauciflora (April to May), melting SGI led to decreases in cumulative PET, where longer melt periods resulted in differences of 2–4 mm compared with $PETQ_{G10}$, increasing to 10–16 mm when compared with $PETQ_{G_{NONE}}$. For the annual water budget, a difference of 10mm can be enough to change a peatland water deficit, to a slight water surplus or net-neutral conditions (Wells et al., 2017). However, a difference of 10mm is also well within the range of error for most water budget studies, and as such its significance should be considered with some caution. Also, similar to the reduced effect discussed with AET, as the SGI becomes discontinuous, lateral melting could lessen the reduction in PET.

Furthermore, SGI free areas can open up over the course of the melt period suggesting that there are spatial differences in both the melt rate and ice thickness. These spatial differences would mean Q_G for peatlands is spatially variable, and possibly AET and PET. Despite these caveats, future studies should focus on incorporating Q_L into Q_G for peatlands that experience more frequent wet and dry cycles to better understand the relative impact of melting SGI on PET and AET.

For this study, it was assumed that evapotranspiration was a function of available energy and atmospheric conditions, and was not limited by moisture. Towards the end of the spring season though, this assumption may not be true, particularly for sites with pronounced microtopography. Figure 6 illustrates that hummocks were consistently drier than hollows due to their elevated position. This means SGI would be deeper relative to the surface and may be insulated by the overlying peat layers, leading to slower melt rates in hummocks compared with hollows such as between the May 3–9 ice survey (Figure 2). If the air during the spring is particularly dry, then water above the ice may evaporate more quickly than the melting SGI can supply liquid water. Such a scenario (Kingsbury & Moore, 1987) could slow melting, reduce the Q_G , and lead to desiccation. Similar results were shown under unsaturated conditions by Thompson and

Waddington (2013) who further suggested that the desiccation could be due to moisture migration within the microtopographic feature (Nagare et al., 2012). Whereas a reduction in melt may increase PET due to a smaller Q_G and increased available energy, there may not be an increase in AET. The reduction in VMC would lower the unsaturated hydraulic conductivity of the peat, and the moss would not be able to meet evaporative demand (McCarter & Price, 2014) possibly leading to desiccation. Surface desiccation was observed in some hummocks, with associated low (<5%) VMC during the 2017 spring at Pauciflora; however, the site scale impact was likely minimal. Furthermore, the IWE (139 mm) exceeded PET (44 mm) during the melt period, indicating SGI would promote wet rather than dry conditions at Pauciflora. Unfortunately, there was insufficient data overlap between the AET dataset and spring SGI melt to assess the impact of SGI melt on AET across multiple springs. Future studies should investigate whether or not the melting of SGI reduces AET significantly below PET.

4.4 | SGI's role in a headwater catchment peatland in the WBP

The role of SGI at Pauciflora may be most pronounced during the spring, when it can act as a moisture source and constraint on evapotranspiration. SGI melt did not begin until after the snow that fell on April 16 had melted, which resulted in low infiltrability for the peatland, and subsequently less snowmelt water likely remained within the peatland (Ireson et al., 2015; Watanabe et al., 2013). This suggests that for the 2017 spring, most of the 64mm of SWE was likely lost to run-off, evaporation, and sublimation and had a minimal contribution to early plant photosynthesis. The presence of SGI close to the peat surface (Figure 4) and a subsequent high water table (Figure 5a) created wet conditions, elevating near surface soil moisture conditions (Figure 6). Hummocks remained drier compared with hollows and lawns due to their elevated positions above the water table and SGI. As the SGI melted, the increase in water table depth was minimal (≈ 3 cm below the peat surface in hollows), because SGI was converted to liquid water. The high amount of water released in the upper 30 cm supplemented any snowmelt loss from the peatland, reducing the potential for moisture stress conditions for surface vegetation. This amount of water also supplements any snowmelt that was lost from the peatland. In this way, the melting SGI acted as a supplier of water for peatland vegetation, particularly in the absence of precipitation. This available water also resulted in evapotranspiration rates occurring closer to potential rates, which were lowered by reduced available energy from melting SGI (Figure 8). SGI acted both as an enhancement due to its supply of water and a constraint due to suppressed soil temperatures on evapotranspiration (Figure 7).

The water released by melting SGI is not “new” water being added to the peatland, and its position relative to the surface is likely a function of the antecedent moisture conditions prior to SGI formation. Lack of a SGI layer close to the peatland surface prior to melt may be due to a lower water table at the time of freezing. The coincidence of a low SGI layer and a drier spring may lead to early season moisture stress for peatland vegetation. SGI keeps a water source close to the

surface, reducing the effects of water table drawdown. For our study area, a poor fen, Wells et al. (2017) reported a steady increase in the water table over the winter from 2011 to 2012. Missing data over subsequent winters however limited these observations to only one winter. In a western boreal forest wetland basin, Price and FitzGibbon (1987) found that whereas fens maintained water table levels at the freezing front, bogs experienced some water table drawdown over winter. Conversely, Kingsbury and Moore (1987) found that a “dehydrated” layer formed beneath the SGI but above the lower water table in a subarctic fen. This highlights that the role of SGI as a source of water may be more relevant for bogs than fens in the WBP. For a bog, any water table drawdown, over the winter after SGI formation, would not be replenished until after snowmelt, increasing the importance of SGI melt water.

This work was completed at a headwater catchment within the WBP, and as such the role of SGI in the WBP may differ depending on the amount of snowmelt, and peatland location within the landscape. At the individual peatland scale, SGI importance to peatland vegetation may be higher when there is less snowmelt. Its contribution of a large amount of water to the surface in one event may help offset the effects of a drier spring. If there is little SGI present, and low water tables (i.e., increased peatland storage capacity) at the beginning of spring, this may decrease snowmelt run-off from the peatland. Given the potential hydrological importance of headwater peatlands such as Pauciflora (Wells et al., 2017) and the “downstream” impacts of headwater peatlands, this could mean that the presence and persistence of SGI in headwater catchment peatlands may impact the hydrological regime of lower elevation ecosystems.

5 | CONCLUSIONS

This study highlights the potential roles of SGI during melt in a WBP peatland. Microtopography and soil moisture had limited influence on SGI melt as evidenced by similar melt rates across the site. The role of peatlands as a source area for run-off in this environment is aided in part by the presence of SGI due to its role in elevating the water table after the snowmelt period. The large amount of water released by melting SGI supplies water close to the surface while melting reduces PET. This lowers the upper limit of what AET could be, despite keeping AET close to PET, and reduces overall evapotranspiration rates from a peatland. This may be a mechanism that allows peatlands to persist in the subhumid WBP. Further research is needed to assess how these roles may vary across different peatland types, and under wet and dry cycles. Furthermore, the spatial characteristics of SGI melt are poorly understood, and an investigation into the controls on SGI melt may help elucidate the persistence of SGI influence on evapotranspiration during the spring. Finally, future modelling efforts should investigate how SGI might respond to a warmer climate and how that might impact its role within peatlands in the WBP. This work ultimately has improved our understanding of the role of SGI in WBP peatlands and can serve as a baseline comparison for future studies.

ACKNOWLEDGMENTS

The authors wish to thank C. Van Beest, T. Gauthier, N. Popovic, A. Green, and E. Kessel for field assistance, J. Elliot for providing advice in R studio, and J. Sherwood for comments and suggestions on an early version of this manuscript. We gratefully acknowledge funding from a grant Richard M. Petrone from the National Science and Engineering Research Council (NSERC) of the Canada Collaborative Research and Development Program, co-funded by Suncor Energy Inc., Imperial Oil Resources Limited, Shell Canada Energy, and Boreal Water Futures.

AUTHOR CONTRIBUTIONS

B. Van Huizen completed the study design, data analysis, generated the original ideas of the role of seasonal ground ice in the Western Boreal Plains, and wrote the first draft of the manuscript. R. Petrone contributed to the study design and provided feedback on the analysis and writing of the manuscript. J. Price, W. Quinton, and J. Pomeroy also provided feedback on the analysis and interpretation.

DATA AVAILABILITY STATEMENT

The data that support the findings of this study are available from the corresponding author upon reasonable request.

ORCID

Brandon Van Huizen  <https://orcid.org/0000-0001-8422-7592>

Richard M. Petrone  <https://orcid.org/0000-0002-9569-4337>

Jonathan S. Price  <https://orcid.org/0000-0003-3210-6363>

William L. Quinton  <https://orcid.org/0000-0001-5707-4519>

John W. Pomeroy  <https://orcid.org/0000-0002-4782-7457>

REFERENCES

- Adams, W. P., & Barr, D. R. (1974). Techniques and equipment for measurement of snowcover, including stratigraphy. *Trent University Department of Geography Occasional Papers*, 3, 11–26 pp.
- Bocking, E., Cooper, D. J., & Price, J. (2017). Using tree ring analysis to determine impacts of a road on a boreal peatland. *Forest Ecology and Management*, 404(April), 24–30. <https://doi.org/10.1016/j.foreco.2017.08.007>
- Boelter, D. H. (1969). Physical properties of peats as related to degree of decomposition. *Proceedings of American Soil Science Society*, 33, 606–609.
- Brown, S. M., Petrone, R. M., Mendoza, C., & Devito, K. J. (2010). Surface vegetation controls on evapotranspiration from a sub-humid Western Boreal Plain wetland. *Hydrological Processes*, 24(8), 1072–1085. <https://doi.org/10.1002/hyp.7569>
- Burba, G., Schmidt, A., Scott, R. L., Nakai, T., Kathilankal, J., Fratini, G., ... Velgersdyk, M. (2012). Calculating CO₂ and H₂O eddy covariance fluxes from an enclosed gas analyzer using an instantaneous mixing ratio. *Global Change Biology*, 18(1), 385–399. <https://doi.org/10.1111/j.1365-2486.2011.02536.x>
- Cheng, G., & Chamberlain, E. J. (1988). Observations of moisture migration in frozen soils during thawing. *Canadian Geotechnical Journal*, 17, 54–60. <https://doi.org/10.1139/t80-005>

- Devito, K. J., Creed, I. F., & Fraser, C. J. D. (2005). Controls on runoff from a partially harvested aspen-forested headwater catchment, Boreal Plain, Canada. *Hydrological Processes*, 19(1), 3–25. <https://doi.org/10.1002/hyp.5776>
- Elmes, M., Thompson, D., Sherwood, J., & Price, J. (2018). Hydrometeorological conditions preceding wildfire, and the subsequent burning of a fen watershed in Fort McMurray, Alberta, Canada. *Natural Hazards and Earth System Sciences*, 18, 157–170.
- Farouki, O. T. (1981). Thermal properties of soils. In *Physics of Plant Environment* (2nd ed.). Hanover, N.H: United States Army Corps of Engineers. <https://doi.org/10.4236/ojss.2011.13011>
- FitzGibbon, J. E. (1981). Thawing of seasonally frozen ground in organic terrain in central Saskatchewan. *Canadian Journal of Earth Sciences*, 18(9), 1492–1496. Retrieved from: <https://doi.org/10.1139/e81-139>
- Goetz, J. D., & Price, J. S. (2015). Role of morphological structure and layering of *Sphagnum* and *Tomenthypnum* mosses on moss productivity and evaporation rates. *Canadian Journal of Soil Science*, 95(2), 109–124. <https://doi.org/10.4141/cjss-2014-092>
- Goodbrand, A., Westbrook, C. J., & van der Kamp, G. (2018). Hydrological functions of a peatland in a boreal plains catchment. *Hydrological Processes*, 33, 562–574. <https://doi.org/10.1002/hyp.13343>
- Gorham, E. (1991). Northern peatlands: Role in the carbon cycle and probably responses to climate warming. *Ecological Applications*, 1(2), 182–195. <https://doi.org/10.2307/1941811>
- Granger, R. J. (1989). An examination of the concept of potential evaporation. *Journal of Hydrology*, 111(1–4), 9–19. [https://doi.org/10.1016/0022-1694\(89\)90248-5](https://doi.org/10.1016/0022-1694(89)90248-5)
- Granger, R. J., Gray, D. M., & Dyck, G. E. (1984). Snowmelt infiltration to frozen Prairie soils. *Canadian Journal of Earth Sciences*, 21(6), 669–677. <https://doi.org/10.1139/e84-073>
- Halliwell, D. H., & Rouse, W. R. (1987). Soil Heat Flux in Permafrost: Characteristics and Accuracy of Measurement. *Journal of Climatology*, 7(6), 571–584. <https://doi.org/10.1002/joc.3370070605>
- Hayashi, M. (2013). The cold vadose zone: Hydrological and ecological significance of frozen-soil processes. *Vadose Zone Journal*, 12(4). <https://doi.org/10.2136/vzj2013.03.0064>
- Hayashi, M., Goeller, N., Quinton, W., & Wright, N. (2007). A simple heat conduction method for simulating the frost-table depth in hydrological models. *Hydrological Processes*, 21(19), 2610–2622. <https://doi.org/10.1002/hyp>
- Hayward, P. M., & Clymo, R. S. (1982). Profiles of Water Content and Pore Size in *Sphagnum* and Peat, and their Relation to Peat Bog Ecology. *Proceedings of the Royal Society B: Biological Sciences*, 215(1200), 299–325. <https://doi.org/10.1098/rspb.1982.0044>
- Hedstrom, N. R., & Pomeroy, J. W. (1998). Measurements and modelling of snow interception in the boreal forest. *Hydrological Processes*, 12(10–11), 1611–1625. [https://doi.org/10.1002/\(SICI\)1099-1085\(199808/09\)12:10<1611::AID-HYP684>3.0.CO;2-4](https://doi.org/10.1002/(SICI)1099-1085(199808/09)12:10<1611::AID-HYP684>3.0.CO;2-4)
- Ireson, A. M., Barr, A. G., Johnstone, J. F., Mamet, S. D., van der Kamp, G., Whitfield, C. J., ... Sagin, J. (2015). The changing water cycle: The Boreal Plains ecozone of Western Canada. *Wiley Interdisciplinary Reviews Water*, 2(5), 505–521. <https://doi.org/10.1002/wat2.1098>
- Jiang, R., Gan, T. Y., Xie, J., Wang, N., & Kuo, C. (2017). Historical and potential changes of precipitation and temperature of Alberta subjected to climate change impact: 1900–2100. *Theoretical and Applied Climatology*, 127, 725–739. <https://doi.org/10.1007/s00704-015-1664-y>
- Jones, M., Castonguay, M., Nasr, M., Ogilvie, J., & Arp, P. A. (2014). Modeling hydrothermal regimes and potential impacts of climate change on permafrost within the South Mackenzie Plain, Northwest Territories, Canada. *Ecoscience*, 21(1), 21–33. <https://doi.org/10.2980/21-1-3663>
- Kaimal, J. C., & Finnigan, J. J. (1994). *Atmospheric boundary layer flows: Their structure and measurement*. New York, USA: Oxford University Press.
- Kingsbury, C. M., & Moore, T. R. (1987). The freeze-thaw cycle of a subarctic fen, northern Quebec, Canada. *Arctic and Alpine Research*, 19(3), 289–295.
- Kleinen, T., Brovkin, V., & Schuldt, R. J. (2012). A dynamic model of wetland extent and peat accumulation: Results for the Holocene. *Biogeosciences*, 9(1), 235–248. <https://doi.org/10.5194/bg-9-235-2012>
- Kljun, N., Calanca, P., Rotach, M. W., & Schmid, H. P. (2004). A simple parameterisation for flux footprint predictions. *Boundary-Layer Meteorology*, 112(3), 503–523. <https://doi.org/10.1023/B>
- Lafleur, P. M., McCaughey, J. H., Joiner, D. W., Bartlett, P. A., & Jelinski, D. E. (1997). Seasonal trends in energy, water, and carbon dioxide fluxes at a northern boreal wetland. *Journal of Geophysical Research-Atmospheres*, 102(24), 29009–29020. <https://doi.org/10.1029/96JD03326>
- Lunardini, V. J. (1981). *Heat transfer in cold climates*. New York: Van Nostrand Reinhold Ltd.
- Marshall, I., Schut, P., & Ballard, M. (1999). Canadian ecodistrict climate normals for Canada 1961–1990. Environment Canada.
- Mbogga, M. S., Wang, T., & Hamann, A. (2010). *A comprehensive set of interpolated climate data for Alberta*. Government of Alberta. Department of Renewable Resources EFM Research Note 01/2010. [https://doi.org/ISBN No.978-0-7785-9183-2](https://doi.org/ISBN%20978-0-7785-9183-2)
- McCarter, C. P. R., & Price, J. S. (2014). Ecohydrology of *Sphagnum* moss hummocks: Mechanisms of capitula water supply and simulated effects of evaporation. *Ecohydrology*, 7(1), 33–44. <https://doi.org/10.1002/eco.1313>
- McClymont, A. F., Hayashi, M., Bentley, L. R., & Christensen, B. S. (2013). Geophysical imaging and thermal modeling of subsurface morphology and thaw evolution of discontinuous permafrost. *Journal of Geophysical Research - Earth Surface*, 118(3), 1826–1837. <https://doi.org/10.1002/jgrf.20114>
- Monteith, J. L. (1965). Evaporation and Environment. In *Symposia of the Society for Experimental Biology* (pp. 205–234).
- Moore, T. R. (1987). Thermal regime of peatlands in subarctic Eastern Canada. *Canadian Journal of Earth Sciences*, 24(7), 1352–1359. <https://doi.org/10.1139/e87-129>
- Moore, T. R., Lafleur, P. M., Poon, D. M. I., Heumann, B. W., Seaquist, J. W., & Roulet, N. T. (2006). Spring photosynthesis in a cool temperate bog. *Global Change Biology*, 12(12), 2323–2335. <https://doi.org/10.1111/j.1365-2486.2006.01247.x>
- Nagare, R. M., Schincariol, R. A., Quinton, W. L., & Hayashi, M. (2012). Effects of freezing on soil temperature, freezing front propagation and moisture redistribution in peat: Laboratory investigations. *Hydrology and Earth System Sciences*, 16, 501–515. <https://doi.org/10.5194/hess-16-501-2012>
- Oke, T. R. (1987). *Boundary layer climates* (2nd ed.). London: Taylor & Francis.
- Petrone, R., Devito, K., & Silins, U. (2008). Importance of seasonal frost to peat water storage: Western Boreal Plains, Canada. In *Groundwater-Surface Water Interaction: Process Understanding, Conceptualization and Modelling (Proceedings of Symposium HS1002at IUGG2007, Perugia, July 2007)* Vol. 321, pp.61–66. Retrieved from <http://www.cabdirect.org/abstracts/20093172603.html>
- Petrone, R. M., Chasmer, L., Hopkinson, C., Silins, U., Landhäusser, S. M., Kljun, N., & Devito, K. J. (2014). Effects of harvesting and drought on CO₂ and H₂O fluxes in an aspen-dominated western boreal plain forest: Early chronosequence recovery. *Canadian Journal of Forest Research*, 45(1), 87–100. <https://doi.org/10.1139/cjfr-2014-0253>
- Petrone, R. M., Devito, K. J., Silins, U., Mendoza, C., Brown, S. C., Kaufman, S. C., & Price, J. S. (2008). Transient peat properties in two pond-peatland complexes in the sub-humid Western Boreal Plain, Canada. *Mires and Peat*, 3, 1–13.
- Petrone, R. M., Silins, U., & Devito, K. J. (2007). Dynamics of evapotranspiration from a riparian pond complex in the Western Boreal Forest, Alberta, Canada. *Hydrological Processes*, 21, 1391–1401. <https://doi.org/10.1002/hyp.6298>

- Price, J., & FitzGibbon, J. E. (1987). Groundwater storage–streamflow relations during winter in a subarctic wetland, Saskatchewan. *Canadian Journal of Earth Sciences*, 24, 2074–2081.
- Price, J. S. (1987). The influence of wetland and mineral terrain types on snowmelt runoff in the subarctic. *Canadian Water Resources Journal*, 12(2), 37–41. <https://doi.org/10.4296/cwrj1202043>
- Redding, T., & Devito, K. (2011). Aspect and soil textural controls on snowmelt runoff on forested boreal plain hillslopes. *Hydrology Research*, 42(4), 250. <https://doi.org/10.2166/nh.2011.162>
- Redding, T. E., & Devito, K. J. (2005). Particle densities of wetland soils in northern Alberta, Canada. *Canadian Journal of Geotechnical Engineering*, 1(86), 57–60. <https://doi.org/10.4141/S05-061>
- Rooney, R. C., Bayley, S. E., & Schindler, D. W. (2012). Oil sands mining and reclamation cause massive loss of peatland and stored carbon. *Proceedings of the National Academy of Sciences of the United States of America*, 109(13), 4933–4937. <https://doi.org/10.1073/pnas.1>
- Rouse, W. R. (1984). Microclimate of arctic tree line 2. Microclimate of Tundra and Forest. *Water Resources Research*, 20(1), 67–73. <https://doi.org/https://doi.org/10.1029/WR020i001p00067>
- Rouse, W. R. (2000). The energy and water balance of high latitude wetlands: Controls and extrapolation. *Global Change Biology*, 6(S1), 59–68. <https://doi.org/10.1046/j.1365-2486.2000.06013.x>
- Runkle, B. R. K., Wille, C., Gazovic, M., Wilmking, M., & Kutzbach, L. (2014). The surface energy balance and its drivers in a boreal peatland fen of northwestern Russia. *Journal of Hydrology*, 511, 359–373. <https://doi.org/10.1016/j.jhydrol.2014.01.056>
- Schippenger, B., & Rydin, H. (1998). Response of photosynthesis of Sphagnum species from contrasting microhabitats to tissue water content and repeated desiccation. *New Phytologist*, 140(4), 677–684. <https://doi.org/10.1046/j.1469-8137.1998.00311.x>
- Smerdon, B. D., Mendoza, C. A., & Devito, K. J. (2008). Influence of sub-humid climate and water table depth on groundwater recharge in shallow outwash aquifers. *Water Resources Research*, 44(8), 1–15. <https://doi.org/10.1029/2007WR005950>
- Smerdon, B. D., & Mendoza, C. A. (2010). Hysteretic freezing characteristics of riparian peatlands in the Western Boreal forest of Canada. *Hydrological Processes*, 24(8), 1027–1038. <https://doi.org/10.1002/hyp.7544>
- Song-Miao, F., Wofsy, S. C., Bakwin, P. S., Jacob, D. J., & Fitzjarrald, D. R. (1990). Atmosphere-biosphere exchange of CO₂ and O₃ in the central Amazon forest. *Journal of Geophysical Research*, 95(D10), 851–864.
- Talamucci, F. (2003). Freezing processes in porous media: Formation of ice lenses, swelling of the soil. *Mathematical and Computer Modelling*, 37(5), 595–602. [https://doi.org/10.1016/S0895-7177\(03\)00053-0](https://doi.org/10.1016/S0895-7177(03)00053-0)
- Thiessen, A. H. (1911). Precipitation averages for large areas. *Monthly Weather Review*, 39, 1082–1084.
- Thompson, C., Mendoza, C. A., & Devito, K. J. (2017). Potential influence of climate change on ecosystems within the Boreal Plains of Alberta. *Hydrological Processes*, 31(11), 2110–2124. <https://doi.org/10.1002/hyp.11183>
- Thompson, C., Mendoza, C. a., Devito, K. J., & Petrone, R. M. (2015). Climatic controls on groundwater–surface water interactions within the Boreal Plains of Alberta: Field observations and numerical simulations. *Journal of Hydrology*, 527, 734–746. <https://doi.org/10.1016/j.jhydrol.2015.05.027>
- Thompson, D. K., & Waddington, J. M. (2013). Wildfire effects on vadose zone hydrology in forested boreal peatland microforms. *Journal of Hydrology*, 486, 48–56. <https://doi.org/10.1016/j.jhydrol.2013.01.014>
- Todd, G. W. (1909). Thermal conductivity of air and other gases.
- van Everdingen, R. (1975). Geocryological terminology. *Canadian Journal of Earth Sciences*, 13, 862–867.
- Vaughan, D. G., Comiso, J. C., Allison, I., Carrasco, J., Kaser, G., Kwok, R., ... Zhang, T. (2013). Observations: Cryosphere. In *Climate Change 2013: The Physical Science Basis. Contribution of Working Group I to the Fifth Assessment Report of the Intergovernmental Panel on Climate Change* (pp.317–382). Cambridge, United Kingdom and New York, NY, USA: Cambridge University Press. <https://doi.org/10.1017/CBO9781107415324.012>
- Waddington, J. M., Morris, P. J., Kettridge, N., Granath, G., Thompson, D. K., & Moore, P. A. (2015). Hydrological feedbacks in northern peatlands. *Ecohydrology*, 8(1), 113–127. <https://doi.org/10.1002/eco.1493>
- Wang, Y., Hogg, E. H., Price, D. T., Edwards, J., & Williamson, T. (2014). Past and projected future changes in moisture conditions in the Canadian boreal forest. *The Forestry Chronicle*, 90(June), 678–691. <https://doi.org/https://doi.org/10.5558/tfc2014-134>
- Warren, R. K., Pappas, C., Helbig, M., Chasmer, L. E., Berg, A. A., Baltzer, J. L., ... Sonnentag, O. (2018). Minor contribution of overstorey transpiration to landscape evapotranspiration in boreal permafrost peatlands. *Ecohydrology*, 11(5), 1–10. <https://doi.org/10.1002/eco.1975>
- Watanabe, K., Kito, T., Dun, S., Wu, J. Q., Greer, R. C., & Flury, M. (2013). Water infiltration into a frozen soil with simultaneous melting of the frozen layer. *Vadose Zone Journal*, 12(1), 0. <https://doi.org/10.2136/vzj2011.0188>
- Wells, C., Ketcheson, S., & Price, J. (2017). Hydrology of a wetland-dominated headwater basin in the Boreal Plain, Alberta, Canada. *Journal of Hydrology*, 547, 168–183. <https://doi.org/10.1016/j.jhydrol.2017.01.052>
- Wells, C. M., & Price, J. S. (2015). A hydrologic assessment of a saline-spring fen in the Athabasca oil sands region, Alberta, Canada—A potential analogue for oil sands reclamation. *Hydrological Processes*, 29(20), 4533–4548. <https://doi.org/10.1002/hyp.10518>
- Whittington, P. N., & Price, J. S. (2006). The effects of water table draw-down (asa surrogate for climate change) on the hydrology of a fen peatland, Canada. *Hydrological Processes*, 2274(November 2008), 2267–2274. <https://doi.org/10.1002/hyp>
- Woo, M., & Xia, Z. (1996). Effects of hydrology on the thermal conditions of the active layer. *Nordic Hydrology*, 27, 129–142. <https://doi.org/10.2166/nh.1996.009>
- Woo, M. K., & Winter, T. C. (1993). The role of permafrost and seasonal frost in the hydrology of northern wetlands in North America. *Journal of Hydrology*, 141(1–4), 5–31. [https://doi.org/10.1016/0022-1694\(93\)90043-9](https://doi.org/10.1016/0022-1694(93)90043-9)
- Wright, N., Hayashi, M., & Quinton, W. L. (2009). Spatial and temporal variations in active layer thawing and their implication on runoff generation in peat-covered permafrost terrain. *Water Resources Research*, 45(5), 1–13. <https://doi.org/10.1029/2008WR006880>
- Young-Robertson, J. M., Ogle, K., & Welker, J. M. (2017). Thawing seasonal ground ice: An important water source for boreal forest plants in Interior Alaska. *Ecohydrology*, 10(3), 1–16. <https://doi.org/10.1002/eco.1796>

How to cite this article: Van Huizen B, Petrone RM, Price JS, Quinton WL, Pomeroy JW. Seasonal ground ice impacts on spring ecohydrological conditions in a western boreal plains peatland. *Hydrological Processes*. 2020;34:765–779. <https://doi.org/10.1002/hyp.13626>